4D Smoothing of Gated SPECT Images Using a Left-Ventricle Shape Model and a Deformable Mesh

Jovan G. Brankov, *Member, IEEE*, Yongyi Yang, *Senior Member, IEEE*, Bing Feng, *Member, IEEE,* Michael A. King, *Senior Member, IEEE*, and Miles N. Wernick, *Senior Member, IEEE*

***Abstract*--We present a new 4D smoothing method for cardiac-gated SPECT. The method uses motion-compensated spatio-temporal filtering, based on motion estimated using a global left-ventricular shape model, and a deformable mesh, which accounts for myocardial brightening. The high noise levels in gated SPECT can cause difficulties for motion estimation methods that are based on local information, such as optical-flow techniques. In the proposed approach, we mitigate these problems by using a global shape model of the left ventricle (LV). This model is used to generate a volumetric mesh which is deformed from frame to frame to track myocardium motion through time. As opposed to surface based motion estimation, which follow the motion trajectories of points on the LV surface, our approach is a volumetric method, which aims to follow points within the myocardium. Therefore the method is explicitly designed to track and maintain the relative position of myocardial tissue elements. In addition, the proposed motion estimation allows incorporation of myocardial brightening, which is an artifact of the partial volume artifact, but plays a useful role in clinical assessment of wall thickening. Clinical SPECT data are used in this preliminary study to demonstrate the proposed method.**

I. Introduction

In our prior work [1] we developed a framework for 4D (3D space plus 1D time) processing, reconstruction and motion estimation of gated cardiac SPECT images. There we proposed a mesh-based approach, which models the myocardium and its motion efficiently by using a deformable mesh model (DMM). The DMM approach involves partitioning of the image domain into a collection of non-overlapping patches, called *mesh elements*, then describing the motion over each element through interpolation from the nodal displacement.

In this work we further refine the most critical step in this framework, which is motion estimation, and apply the method to clinical data. Specifically, we introduce a global shape model of the left ventricle, which helps to mitigate the effect of noise in the motion estimation step. The proposed method also preserves myocardial brightening, an artifact of the partial volume effect, which clinicians find practically useful as a way to assess wall thickening.

In the proposed method, we incorporate prior knowledge of the left ventricular (LV) shape into the motion estimation step. LV shape estimation is very mature, and has been widely applied in gated SPECT clinical SPECT software to estimate LV ejection fraction (LVEF), wall motion, etc. (e.g., [2, 3]). However, to our knowledge, LV shape models have not been employed as a foundation for 4D image reconstruction in gated SPECT.

Our method begins by developing a global LV shape model to locate and describe the endocardial and epicardial surfaces of the LV in the gated frames (see Figure 1). The resulting surface model is used to generate a volumetric mesh model, which is then deformed from frame to frame to track myocardial motion through the image sequence. We then use this mesh to guide motion-compensated 4D smoothing. In this paper, we use motion-compensated averaging of all the frames, adjusted for the partial volume effect, while preserving motion through motion compensation.

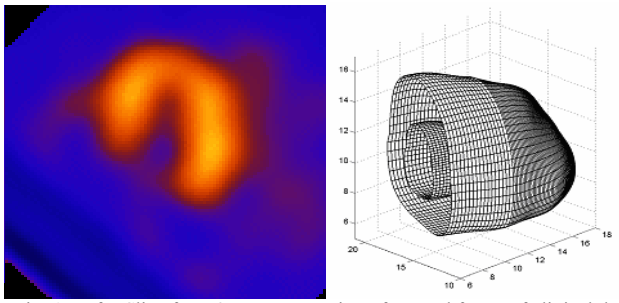

Fig. 1. Left: Slice from 3D reconstruction of a gated frame of clinical data; Right: 3D rendering of the myocardial surfaces detected from this 3D image.

As opposed to surface-based motion estimation, which follows the motion trajectories of points on the LV surfaces [4, 5], our approach is a dense-field, volumetric approach, which

This work was supported by NIH/NHLBI Grant HL65425

J. G. Brankov is with the Department of Electrical and Computer Engineering, Illinois Institute of Technology, 3301 S. Dearborn St., Chicago, IL 60616 USA (telephone: 312-567-8819, e-mail: brankov@iit.edu).

Y. Yang is with the Department of Electrical and Computer Engineering, Illinois Institute of Technology, 3301 S. Dearborn St., Chicago, IL 60616 USA (telephone: 312-567-3423, e-mail: yy@ece.iit.edu).

B. Feng is with University of Massachusetts Medical Center, Worcester, MA, USA (e-mail: Bing.Feng@umassmed.edu).

M. A. King is with University of Massachusetts Medical Center, Worcester, MA, USA (telephone: 508-856-4255, e-mail: Michael.King@umassmed.edu).

M. N. Wernick is with the Department of Electrical and Computer Engineering and the Department of Biomedical Engineering, Illinois Institute of Technology, 3301 S. Dearborn St., Chicago, IL 60616 USA (telephone: 312-567-8818, e-mail: wernick@iit.edu).

follows points within the myocardium. Therefore the proposed method is explicitly designed to maintain the relative positions of myocardium tissue elements. In addition, the method accounts for myocardial brightening [6, 1], an effect that violates the constant-intensity assumption of classical motion-estimation algorithms, leading to suboptimal results.

II. METHODS

In this section we describe main four steps of the proposed 4D smoothing method: initial mesh generation, dense motion filed estimation given DMM, procedure to obtain DMM witch tracks myocardium and spatio-temporal filtering which uses the dense motion field obtained by DMM.

A. Mesh generation

Here we describe the initial mesh-generation procedure used in proposed method. First, segmentation is performed on a reconstructed spatially-smoothed summed image, i.e., all projections are summed followed by filtered backprojection reconstruction (or alternatively other reconstruction algorithm) and spatial low-pass filtering. The LV surfaces are determined using a combination of cylindrical and spherical coordinate systems [7]. This method has been demonstrated to be robust to noise using clinical SPECT data. Figure 1 shows an example obtained by applying this method to clinical gated SPECT data.

To reduce the model complexity, the surface model shown in Figure 1 is next downsampled to obtain a surface model such as that shown in Figure 2(a). Next, the surface control points (nodes) are connected by Delaunay triangulation. This forms a partitioning of the myocardium into a collection of M tetrahedrons. Note that *all* tetrahedrons are located between the endocardial and epicardial surfaces.

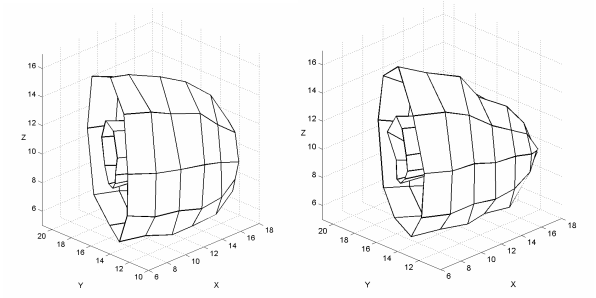

(a) (b)

Fig. 2. Deformable mesh at end diastole and end systole.

B. Deformable mesh for motion representation

Here we will describe how a DMM was used to describe the cardiac motion in a gated SPECT image sequence. The mesh elements in a deformable mesh are allowed to deform over time (as illustrated in Figure 2). The motion field is then interpolated from the motion (displacement) of the mesh nodes.

Let $X^k = \{\mathbf{x}_1^{(k)}, \ldots, \mathbf{x}_N^{(k)}\}$ be the set of locations of the N nodes that constitute the mesh for frame k, and let $X^l = \{\mathbf{x}_1^{(l)}, \ldots, \mathbf{x}_N^{(l)}\}$ be the set of corresponding nodal positions for frame l. The nodal displacement is then given as $\mathbf{d}_n^{k\to l} = \mathbf{x}_n^{(l)} - \mathbf{x}_n^{(k)}$. This vector represents the displacement of node n from frame k to frame l.

Here we can define a set of all displacement vectors from frame k, to frame l as $\mathbf{D}^{k\to l} = \{\mathbf{d}_1^{k\to l}, \ldots, \mathbf{d}_N^{k\to l}\}$ which is a mesh representation of the MF.

The image motion at any spatial location $\mathbf{x}$, denoted by $\mathbf{d}^{k\to l}(\mathbf{x})$, is then interpolated from the set of nodal displacement vectors $\mathbf{D}^{k\to l}$. That is, for $\mathbf{x}$, the mesh representation leads to

$$\mathbf{d}\left(\mathbf{x}; \mathbf{D}^{k\to l}\right) = \sum_{n=1}^{N} \mathbf{d}_n^{k\to l} \phi_n(\mathbf{x}), \quad (1)$$

where $\phi_n(\mathbf{x})$ is the interpolation basis function associated with the *n*th node. In this paper a linear interpolation functions are used, therefore, the support of $\phi_n(\mathbf{x})$ is extending only to a mesh elements attached to *n*th node.

C. Mesh-based motion estimation

The goal of motion estimation is to determine the motion field (MF) $\mathbf{d}^{k\to l}(\mathbf{x})$, i.e., the relative displacement between any point $\mathbf{x}$ in the current frame k and its corresponding position in target frame l. The MF, if accurate, should allow the target frame to be well-estimated by a motion-compensated version of the current frame, i.e., $f_k\left(\mathbf{x} + \mathbf{d}^{k\to l}(\mathbf{x})\right)$ should be a good match to $f_l(\mathbf{x})$.

Given mesh model nodal positions for frame k and l, the goal is to determine their corresponding locations or equivalently displacement vectors, $\mathbf{D}^{k\to l}$. We accomplish this by minimizing a matching criterion defined as:

$$E\left(\mathbf{D}^{k\to l}\right) = \frac{1}{2}\sum_{m=1}^{M}\left[\int_{D_m}\left[f_k\left(\mathbf{x} + \mathbf{d}\left(\mathbf{x}; \mathbf{D}^{k\to l}\right)\right) - f_l(\mathbf{x}) \cdot \frac{volume\left(D_m^k\right)}{volume\left(D_m^l\right)}\right]^2 d\mathbf{x}\right] \quad (2)$$

where D_m, $m = 1, 2, \cdots, M$ is a collection of tetrahedrons (partitioning of the myocardium) and $\mathbf{d}\left(\mathbf{x}; \mathbf{D}^{k\to l}\right)$ is defined as in Eq. (1). This model reflects the linear change [6] in brightness as the myocardium contracts.

Objective function $E\left(\mathbf{D}^{k\to l}\right)$ in Eq. (2) is an adaptation of an algorithm proposed by Wang and Lee [8] modified to account for the brightening effect. In the same paper one can find analytical expression of the gradient of the $E\left(\mathbf{D}^{k\to l}\right)$ functional with respect to nodal displacement $\mathbf{d}_n^{k\to l}$. This analytical gradient expression is used in iterative gradient-descent minimization algorithm of Eq. 2 with a line search algorithm to determine optimal descending step.

Next we describe how the DMM is obtained for the whole image sequence. First, the image sequence is reconstructed by

filtered backprojection reconstruction (or alternatively another reconstruction algorithm that does not perform temporal smoothing) followed by spatial low-pass filtering. Next, we assign to the first and second frame an initial mesh structure obtained as described in Sect. 2.1. Now we continue by minimizing matching criterion, $E\left(\mathbf{D}^{1\to 2}\right)$, for these two frames. The newly obtained mesh structure for the second frame is assigned to the third frame and further deformed by minimizing $E\left(\mathbf{D}^{2\to 3}\right)$. The same procedure is continued through the sequence until the last frame is reached, i.e., $E\left(\mathbf{D}^{K-1\to K}\right)$ is minimized, where K is the number of frames. At this point all frames have assigned mesh structure. Now we continue with deformations using the fact that the gated image sequence is a loop, i.e., the frame following the last frame is the first frame. Thus, the mesh structure for the first frame is deformed by minimizing $E\left(\mathbf{D}^{K\to 1}\right)$, and subsequently we minimize $E\left(\mathbf{D}^{1\to 2}\right)$ and so on. This cycling through the image sequence in carried on until a stable solution is reached, i.e., until there is no significant change in mesh structure at any frame. We found, empirically, that this is usually achieved in 5-10 iterations through the whole sequence.

Having obtained the mesh structure for every image in the sequence, we can now obtain the motion field at any spatial location between any two frame by using Eq. (1).

Examples of mesh structures for two frames, for the heart at end diastole and end systole, are shown in Figure 2 and Figure 3. Figure 2 shows only the mesh structures whereas Figure 3 shows mesh structures with estimated myocardial surfaces overlying two perpendicular slices of volumetric data.

D. Accurate Pixel-Based Spatio-Temporal Filter

In this work we used a separable spatio-temporal filter. First, using the DMM for MF estimation, we define the following motion-compensated temporal averaging in the pixel domain:

$$\hat{f}_k(\mathbf{x}) = \frac{1}{K}\sum_{l=1}^{K} f_l\left(\mathbf{x}-\mathbf{d}\left(\mathbf{x};\mathbf{D}^{k\to l}\right)\right)\cdot\left(1-div\left(\mathbf{d}\left(\mathbf{x};\mathbf{D}^{k\to l}\right)\right)\right) \qquad (3)$$

where $div\left(\mathbf{d}\left(\mathbf{x};\mathbf{D}^{k\to l}\right)\right)$ denotes the divergence of the motion vector field (compensation for brightening) and K is the number of frames. Without motion compensation, this averaging would yield a completely *motionless* image of the heart.

After temporal filtering, the image sequence was spatially filtered with a Butterworth filter of order 4 and cutoff frequency of 0.45.

E. Method summary

The proposed method consists of following steps:

- Mesh generation
  - Summed image reconstruction (FBP);
  - Spatial low-pass filtering;
  - Surface detection [7];
  - Surface down-sampling;
  - Delaunay triangulation;
- Mesh deformation
  - Image sequence reconstruction (FBP)
  - Spatial low-pass filtering;
  - Minimization of Eq. (2) assuming a circular sequence;
- Motion field interpolation; Eq. (1)
- Spatio-Temporal Filtering
  - Temporal averaging as in Eq. (3);
  - Spatial low-pass filtering.

III. RESULTS

The proposed method was tested on several sets of clinical SPECT data. The results shown here are for a female at rest with a perfusion defect in the right coronary artery (RCA). The data were reconstructed on 64x64 grids from 120 projections. The pixel size was 6.34 mm and the FOV was 27.80cm.

In mesh generation and motion estimation step images were reconstructed by FBP followed by spatially filtering with Butterworth filter of order 4 and cutoff frequency of 0.3.

Estimated DMMs for two perpendicular slices of the clinical data are presented in Figure 3. For better visualization, a smooth surface, obtained from DMM by spline interpolation, is presented as well. One can note excellent agreement between the estimated DMM myocardium surface and the volumetric data intensity. This even more evident if one views the cines of deformable mesh at: http://www.ipl.iit.edu/brankov/MIC04/.

Results, for visual assessment of spatio-temporal processed images are shown in Figure 4. For comparison we also showed results obtained by a method used in clinical practice at the University of Massachusetts. In this method, a spatial Butterworth filter of order 4 and cutoff 0.22, is applied, as well as a temporal filter with impulse response {1, 2, 1}/4. We will refer to this as the 121 method. Since 4D reconstruction results for gated cardiac perfusion studies are difficult to demonstrate in a printed paper, the reader is encouraged to view the cines at the web page referred to earlier.

The cines, as well as Figure 4, suggest that the proposed method reduces noise effectively while preserving myocardium motion and brightening which is encouraging, since we have applied a strongest temporal filter, temporal averaging, adjusted for the partial volume effect. Note that this temporal filter without motion compensation would yield a completely *motionless* image of the heart.

To obtain a preliminary quantitative analysis, we compared the proposed method with the 121 method on the basis of maximum brightening of the myocardium and estimated LV ejection fraction (EF), two features that can be corrupted by inappropriate temporal processing. EF fraction was estimated using the method proposed in [7]. In this quantitative comparison results, shown in Table 1, two case studies are presented, as mentioned earlier: a female with defect in the RCA and a healthy male. The results suggest that the proposed method preserves both features well even though image noise is reduced.

Our next step will be to conduct a more complete and rigorous quantitative evaluation of algorithm performance, including perfusion-defect detectability. We hypothesize that

defect detection will be improved because our method appears to require less spatial smoothing at a given variance level in the images.

TABLE 1.
QUANTITATIVE COMPARISON

Female - with RCA defect	Maximum brightness - systole/diastole	LVEF
121 method	1/0.7703	58.3%
Proposed method	1.04/0.7789	56.8%

Male - healthy	Maximum brightness - systole/diastole	LVEF
121 method	1/0.875	51.4%
Proposed method	1.08/0.876	51.9%

IV. REFERENCES

[1] J. G. Brankov, Y. Yang, M. N. Wernick, and M. V. Narayanan, "Motion-compensated 4D processing of gated SPECT perfusion studies," *Conf. Record of the 2002 IEEE Nucl. Sci. Symp. & Med. Imaging Conf*, vol. 3, pp. 1380-1384, 2002.

[2] E. P. Ficaro, *The User's Manual for 4D-MSPECT,* 2002. Ref Type: Pamphlet

[3] W. Schaefer, C. S. Lipke, B. Nowak, H. J. Kaiser, P. Reinartz, A. Buecker, G. Krombach, U. Buell, H. P. Kuhl, "Validation of QGS and 4D-MSPECT for quantification of left ventricular volumes and ejection fraction from gated 18F-FDG PET: comparison to cardiac MRI," *J. Nucl. Med*., vol. 45, pp. 74-79, 2004.

[4] J. Declerck, J. Feldmar, and N. Ayache, "Definition of a four-dimensional continuous planisferic transformation for the tracking and the analysis of the left-ventricle motion," *Med. Image Anal*., vol. 2, no. 2, pp. 197–213, June 1998.

[5] E. Bardinet, N. Ayache, and L. D. Cohen, "Tracking and motion analysis of the left ventricle with deformable superquadrics," *Med. Image Anal*., vol. 1, no. 2, pp. 129-150, June 1996.

[6] J. R. Galt *et al. IEEE Trans. Med. Imaging* vol. 9 144 -150.

[7] T. L. Faber, C. D. Cooke, J. W. Peifer, R. I. Pettigrew, J. P. Vansant, J. R.Leyendecker, and E. W. Garciar, "Three-Dimensional displays of left ventricular epicardial surface from standard cardiac SPECT perfusion quantification techniques," *J. Nucl. Med*., vol. 36, no. 4, pp. 697-703, Apr. 1995.

[8] Y. Wang and O. Lee, "Active mesh - A feature seeking and tracking image sequence representation scheme," *IEEE Trans. Image Processing* vol. 3 pp. 610-624, 1994.

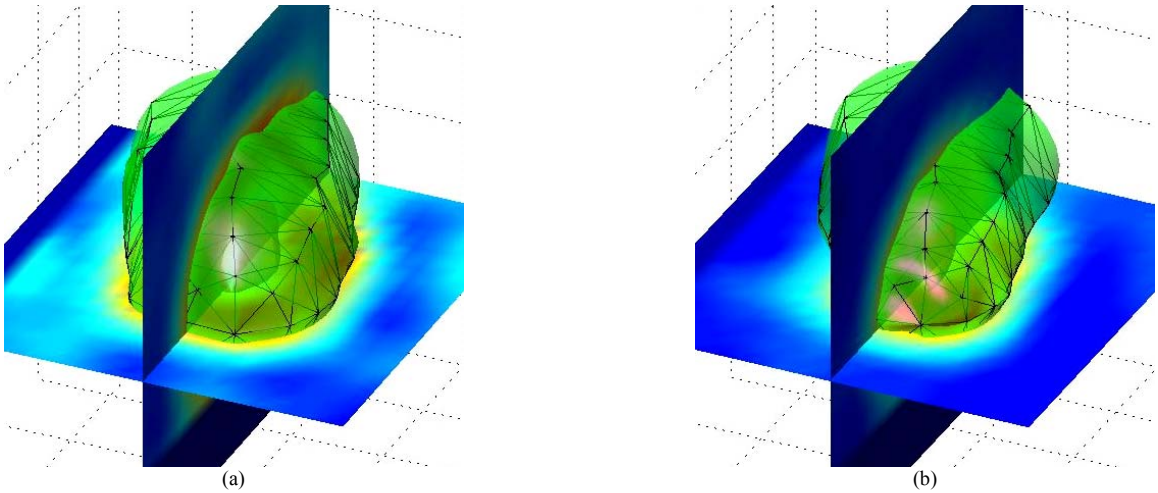

(a) (b)

Fig. 3. Deformable mesh model (wire structure) and interpolated smooth surface at (a) end diastole and (b) end systole overlaying two slices through the volumetric data. Note that the interpolated surface closely follows the myocardium boundary.

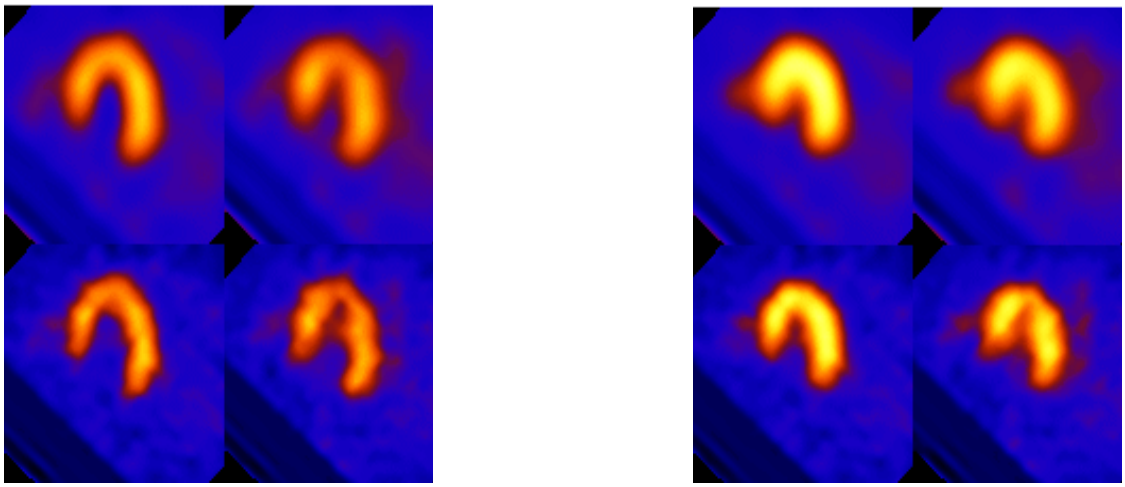

(a) (b)

Fig. 4. Post reconstruction processed clinical data for a female at rest with a perfusion defect in the right coronary artery; (a) end diastole, (b) end systole; Upper row: typical clinical procedure (121); Lower row: proposed method.